Aalborg Universitet

Stored Energy Balance for Distributed PV-Based Active Generators in an AC Microgrid

Aldana, Nelson Leonardo Diaz; Wu, Dan; Dragicevic, Tomislav; Vasquez, Juan Carlos; Guerrero, Josep M.

Stored Energy Balance for Distributed PV-Based Active Generators in an AC Microgrid

Nelson L. Diaz, Dan Wu, Tomislav Dragicevic, Juan C. Vasquez, and Josep M. Guerrero

Abstract—In this paper, a decentralized strategy based on fuzzy logic is proposed for balancing the state of charge of the energy storage units for distributed PV-based active generators. The proposed method, weights the action of conventional droop control loops for privileging the charge of the energy storage unit with the smallest state of charge or force a faster discharge of the energy storage system with the biggest state of charge. The units are self-controlled by using local variables, hence, the microgrid can operate without relying on communication systems. The proposed strategy is completely expandable and can be applied to a several number of power generators interconnected in a microgrid. Frequency and voltage bus signaling is used in order to coordinate the control operation mode between units. Simulation results in a low-voltage, three-phase, islanded AC microgrid show the feasibility of the proposed method and its applicability even for several active generators.

Index Terms—Active Generators, Droop Control, Fuzzy system, Energy Storage Balance.

I. INTRODUCTION

DURING the last years photovoltaic (PV) generation has emerged as one of the most used renewable energy sources (RES) due to current trend at the reduction on its installation cost [1]. However, the intermittent nature of PV generators, added together with unpredictable load fluctuations, may cause instantaneous power unbalances that affect the operation of the system. Hence, Energy storage systems (ESS) are required to guarantee the operation conditions of the power grid by smoothing the variations of RES [2], [3].

At this sense, a microgrid appears as an effective solution for interconnecting RES, ESS and loads as controllable entities, which may operate in grid-connected or islanded mode, either in AC or DC configuration. Particularly, isolated microgrids play and important role when economic and environmental issues do not allow interconnection with the main power grid [4]. Indeed, isolated microgrids become an additional challenge since the voltage and frequency are not imposed for the main grid. Therefore, all the distributed energy resources (PV and ESS) have to operate in a coordinated way in order to ensure the reliability, security and power stability of the local grid [1], [5].

As a matter of fact, there are two ways of integrating ESS, namely aggregated and distributed [6]. Anyhow, the current trend is oriented to distributed ESS, where an ESS is associated to a RES into an entity commonly denoted as active generator

Nelson L. Díaz, D. Wu, T. Dragicevic, J. C. Vásquez and J. M. Guerrero are with the Department of Energy Technology, Aalborg University, Aalborg, Denmark (e-mail: nda@et.aau.dk, dwu@et.aau.dk, tdr@et.aau.dk, juq@et.aau.dk, joz@et.aau.dk).

Nelson L. Díaz, is also with Universidad Distrital F. J. C., Bogotá, Colombia (e-mail: nldiaza@udistrital.edu.co).
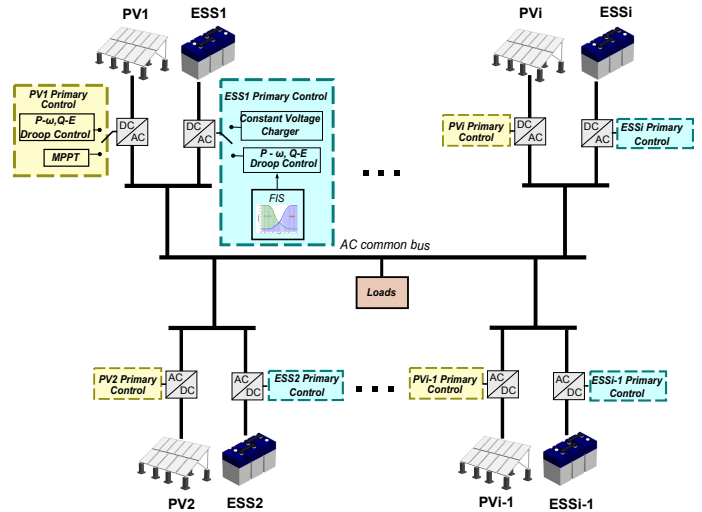
Figure 1. AC microgrid configuration.

(PV+ESS), in order to ensure constant power production based on load requirements, [2], [7].

Fig.1 shows a general scheme for an isolated AC microgrid that is composed by (i) active generators $(PVi + ESSi)$ and loads. Commonly, droop control loops are used to achieve good power sharing between units. Droop control enhance system reliability and expandability, and ensure the robustness without the use of external communication system [1], [8].

Normally, all the power converters operate in voltage control mode (VCM) by following conventional droop control strategy aimed to regulate the bus voltage amplitude and frequency [9]. This approach works when dispatchable power generators are used, but it is not effective for intermittent sources such as PV generators, that are more likely to operate under an algorithm of maximum power tracking (MPPT). At this case, PV generators behave as current sources and operate under current control mode (CCM) [1], [4]. Meanwhile, ESS operate in VCM, being responsible of regulating the bus voltage. Then, under VCM the batteries will be charged or discharged in order to compensate the unbalance between the energy generated by RES and load consumption [10], [11].

Valve regulated lead-acid (VRLA) batteries are commonly used in isolated microgrids, since they offer a good commitment between deep-cycle life, transportability, availability and cost [12], [13]. In that case, the most effective way of charging a VRLA battery is by means of a two stage procedure [12]. First, the ESS are charged based on the unbalanced of energy between RES generation and load consumption, then ESS operate under VCM. Subsequently, when the battery voltage

reach a threshold value known as regulation voltage (V_r), the battery voltage should be kept constant [12]. At this mode, the ESS operate on CCM then the RES should assume the regulation of the common bus by changing their operation mode to VCM. Given the above points, every RES and ESS unit is accompanied by a decision-maker strategy in order to switch between control modes. At this paper, bus-signaling method, by using different bus voltage amplitude/frequency thresholds, is used to trigger the changes at the operation modes for RES and ESS in a coordinated way [1], [10].

Apart from that, when a microgrid is composed by distributed ESS, a coordination to ensure stored energy balance among the units is desired. This coordination aims to avoid deep-discharge in one of the ESS and over-charge in the others. Therefore, during the process of charging, it is expected to prioritize the charge of the unit with the smallest state of charge (SoC), and similarly, during the process of discharging, the unit with the highest SoC should provide more power to the common grid than the others, in order to achieve stored energy balance. In other words, conventional control loops for power sharing at each ESS, may be complemented with stored energy balance strategies [10], [13], [14], [15].

In this paper, a strategy based on a knowledge based fuzzy inference system (FIS) is applied and evaluated for an isolated AC microgrid. In this case, the proposed FIS weight the $P-\omega$ droop coefficients of the droop controllers in accordance with the SoC at each ESS. In Section II the configuration and operation of the microgrid under isolated operation is described. Section III shows the design and operations of the proposed fuzzy strategy for stored energy balance. In section IV explains the reactive power flow control. Section V shows simulation results based on a Simulink model of a a low voltage AC microgrid under islanded operation. The results show the applicability and advantages of the proposed strategy.

II. DESCRIPTION OF THE ISOLATED AC MICROGRID

In order to ensure regulation of the common AC bus voltage, all the units connected to the common bus have to operate in a coordinated way. Due to the inherent power regulation differences between ESS and PV generators, it is not possible that all of them operate under the same control mode [9]. To be more precise, it is expected that PV generators work under a MPPT algorithm in order to obtain the maximum of the available energy. Then, they are regulated based on CCM inner loops. On the contrary, ESS have to operate on VCM inner loop aimed to regulate the bus voltage and frequency. At this stage, the ESS are charged or discharged based on the power unbalance between generated and consumed power [1].

During this stage, the current is limited by droop control loops. However, since a two stage procedure is recommended for charging VRLA batteries (current-limited followed by a constant voltage charger), in order to enhance their lifetime, each ESS should change its operation mode from VCM to CCM when the voltage at the battery array reaches the regulation voltage (V_r) (typically 2.45 ± 0.05 volts/cell) [12]. At this stage, each ESS drains as much power as needed to keep its battery voltage at (V_r) [13]. When distributed ESS are used, the ESS with smaller SoC will continue with the
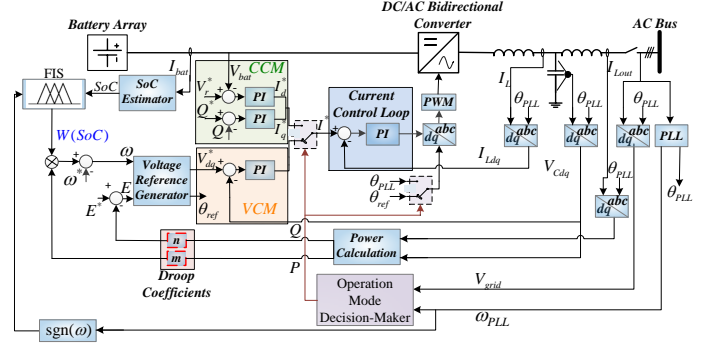
Figure 2. Control diagram for ESS

bus voltage and frequency regulation until it reach the the threshold voltage (V_r). Finally, all the ESS will change its operation mode from VCM to CCM.

At this point, for ensuring bus voltage and frequency regulation, it is necessary that all the RES change their operation mode from CCM to VCM. Consequently, RES change their inner control loops from MPPT to droop control in which the power obtained from RES is limited and equally shared between RES because of the droop control loops. On the contrary, when the RES are not able to support the load consumption ESS change their operation mode from CCM to VCM and RES start to work under MPPT algorithm once again. As a consequence, every ESS and RES requires two inner control loops in order to operate under two different operation modes [13].

A. ESS Unit Operation

Fig. 2 shows the configuration of a ESS unit, which consists of a battery bank, a bidirectional converter, and output filter. The ESS unit is formed by a typical double loop VCM control and a battery voltage regulation double loop CCM [1]. The inner loop VCM controller uses a capacitor voltage controller (V_{Cdq}) and an inductor current (I_{Ldq}) control loop in a dq reference frame. The voltage frequency/amplitude references are calculated by the voltage reference generator, based on the $(P-\omega)$ and $(Q-E)$ droop control loops. Likewise, the inner loop CCM controller uses a battery voltage controller and the same inductor current control loop as the former controller. At this stage, the frequency reference is given by the PLL.

For the transition between operation modes, it is required a decision-maker strategy. At this case, decentralized finite state machines whit two states are used at each ESS unit. The transition between operation modes are triggered by bus voltage/frequency-signaling and the battery array voltage when $V_{bati} = V_r$ for each battery array.

B. PV Unit Operation

Similarly, Fig. 3 shows the configuration of the RES, which consists of PV array, DC/AC converter, output filter, and local controllers. Under CCM, the output power is regulated by the active power reference (P^*) defined by the MPPT algorithm. The reactive power reference (Q^*) is established equal to zero at this case of study. Active and reactive power references together with the capacitor voltage (V_{Cdq}) are used by the current reference generator to calculate the reference current

Figure 3. Control diagram for PV generator

Figure 4. Control curves of the FIS.

(I^*) for the current control loop. The frequency reference is given by the PLL.

On the other hand, inner loop VCM controller is composed by a capacitor voltage controller and the same inner current control loop. The voltage frequency and amplitude references are calculated by the voltage reference generator based on conventional $(P - \omega)$ and $(Q - E)$ droop control loops [8].

For the transition between operation modes, it is also required a decision-maker strategy. Decentralized finite state machines with two states are used at each RES unit. The transition between operation modes are triggered by bus frequency-signaling and power comparison when the MPP power is smaller than the generated power under VCM operation.

It is important to say that smooth transitions between control loops, is achieved by means of enforcing initial conditions of inactive PI controller to the value of the output of the active one [13].

III. FUZZY ADJUSTMENT FOR ESS BALANCE

When batteries are in the process of charge or discharge, the power balance is managed by $P - \omega$ droop control loops [8]. Therefore, the frequency at the common AC bus given by the following equation,

$$\omega = \begin{cases} \omega^* - m \cdot P_{Bati}, & \textbf{If } ESS \textbf{ are } in \ VCM; \\ \omega^* - m \cdot P_{Resi}, & \textbf{If } RES \textbf{ are } in \ VCM. \end{cases} \quad (1)$$

where m is the droop coefficient, ω is the angular frequency at the common bus, ω^* is the reference of the angular frequency, and P_{Bati} is the power driven at each ESS. If we consider differences in the droop coefficients m at each ESS, the battery with the lowest m will inject/extract more power to/from the grid in order to keep the power balance in the microgrid. For that reason, the ESS with the lowest m will be charged or discharged faster than the others.

In light of the above, it is desired that the battery with the lowest SoC is charged faster than all the others for ensuring stored energy balance. Then, a smaller (m) should be assigned to that battery. Likewise, when batteries are supplying power to the common bus, it is desired that a bigger (m) is assigned to the battery with the lowest SoC, in order to prevent a deep discharge and balance the stored energy.

In particular, a FIS can easily summarize all the qualitative knowledge, expressed above. It can cluster the experience and the knowledge of an expert about the expected behavior of the system in order to weight the droop coefficient at

each ESS based on its SoC [10]. Therefore, a fuzzy weight factor $W\left(SoC_{Bati}\right)$, based on a (max-min) Mamdani FIS, is proposed in order to weight the droop coefficient at each ESS, in accordance to its SoC, and considering whether the ESS is being charged or discharged. Particularly, a Mamdani FIS are computationally simple to implement since it is based on basic algebraic and relational operations, or it can even be implemented as a lookup table [16]. Finally, equation (1) is replaced by equation (2) where the fuzzy factor is applied.

$$\omega = \begin{cases} \omega^* - m \cdot W\left(SoC_{Bati}\right) \cdot P_{Bati}, & \textbf{If } ESS \textbf{ are } in \ VCM; \\ \omega^* - m \cdot P_{Resi}, & \textbf{If } RES \textbf{ are } in \ VCM. \end{cases} \quad (2)$$

The FIS uses the SoC and the sign of the frequency deviation (equation (3)) as the inputs, and the weight factor $W(SoC)$ is defined as the output. The SoC is estimated by standard ampere-hour (Ah) counting method as in [1], [13].

$$sgn(\omega) = \begin{cases} 1, & \textbf{If } \omega - \omega^* > 0; \\ -1, & \textbf{If } \omega - \omega^* < 0. \end{cases} \quad (3)$$

To be more precise, the FIS is only active when the ESS are operating in VCM, and it weighs the droop coefficients between 0.1 to 0.9 of their nominal value (Fig. 4). Since the FIS is not based on particular characteristics of a microgrid, it could be applied to microgrids with different power ratings.

IV. REACTIVE POWER SHARING

Conventional $Q - E$ droop controllers are used in order to share the reactive power flow between units in a microgrid. Only the units that are working under VCM will be responsible of the reactive power flow, and it will be equally shared based on equation (4), where (Q_{Bati}) and (Q_{Resi}) represent the reactive power flow at each ESS and RES respectively [8]. In other words, when the ESS are operating in VCM, they are the responsible of reactive power flow and it is equally shared between the ESS units that are under VCM. On the other hand, when all the ESS are operating under constant voltage charge (CCM), all the RES become responsible of the reactive power flow in the microgrid, and the reactive power flow is equally shared between RES units.

$$E = \begin{cases} E^* - n \cdot Q_{Bati}, & \textbf{If } ESS \textbf{ are } in \ VCM; \\ E^* + n \cdot Q_{Resi}, & \textbf{If } RES \textbf{ are } in \ VCM. \end{cases} \quad (4)$$

Since bus voltage-signaling is used for triggering the changes at the decision-makers, a positive droop coefficient (n) is used for ESS and a negative droop coefficient (n) is used for RES. In this way it is possible to identify at each unit, which ones are responsible of the voltage bus regulation

Table I
PARAMETERS OF THE MICROGRID

Parameter	Symbol	Value
	Power Stage	
Nominal Bus Voltage	E^*	$230 * \sqrt{2}$V
Nominal Bus Frequency	ω^*	$2 * \pi * 50$rad/s
Inverter inductors	L	1.8mH
Filter Capacitor	C	$27\mu f$
Nominal Load	P_{Load}	$1600\ W$
	Battery Array	
Nominal Voltage	$Vbat$	672V
Regulation Voltage	V_r	756V
Nominal Battery Capacity	C_{bat}	0.02(Ah)
	Power flow Control	
$(P-\omega)$ Droop Coefficient	m	$1.25 * 10^{-5}$ rd/s/(W)
$(Q-E)$ Droop Coefficient	n	$5 * 10^{-4}$ V/(VAr))
Reactive power Reference	Q^*	0VAr
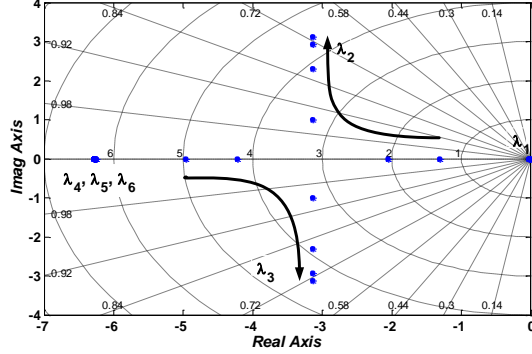
Figure 5. Trace of eigenvalues when SoC_{Bat1} approaches to SoC_{Bat2}
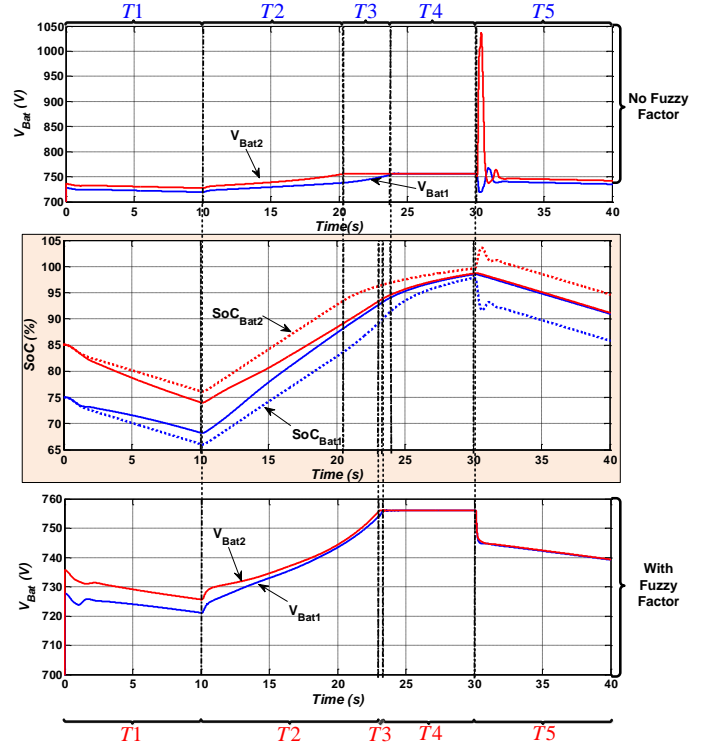

Figure 6. Simulation results with (bottom figures) and without (top figures) fuzzy factor

Table II
CHANGES AT THE OPERATION CONTROL MODE FOR RES AND ESS

	T1	*T2*	*T3*	*T4*	*T5*
RES1	CCM	CCM	CCM	VCM	CCM
RES2	CCM	CCM	CCM	VCM	CCM
ESS1	VCM	VCM	CCM	CCM	VCM
ESS2	VCM	VCM	VCM	CCM	VCM

(ESS or RES). Droop coefficients are calculated for a voltage deviation smaller than 5% at the common bus.

V. SIMULATION RESULTS

A Simulink model of the microgrid has been used in order to test and compare the performance of the microgrid with and without the weight factor $W(SoC)$. The system is designed to supply a nominal resistive load in a balanced three phase system. Table I summarizes the main characteristics of the microgrid. In order to understand the behavior of the microgrid shown in Fig.1, a microgrid with two active power generators (PV+ESS) $(i = 2)$ will be considered at the beginning. Even so, the analysis can be extended to more active generators. Detailed models of the VRLA batteries are used as shown in [13], for simulating the batteries.

A small signal model of the microgrid as proposed in [17] has been used for evaluating the stability of the system. Fig. 5 shows the behavior of the eigenvalues when SoC_{Bat1} approaches to SoC_{Bat2} in accordance to the FIS. A nominal value of $m = 1.25 * 10^{-5} rd/s/(W)$ has been established in order to obtain a maximum damping factor $(\zeta = 0.7)$. It is possible to see that the system remains stable over the entire range of $W(SoC_{Bati})$ while the ESS are equalized.

Fig.6 summarizes some results under changes at the power generated by RES. It is assume that the energy generated by both RES is the same and it changes from $500W$ to $1500W$ at $Time = 10s$ and from $1500W$ to $500W$ at $Time = 30s$. An initial SoC of 75% for battery 1 $(Bat1)$ and 85% for battery 2 $(Bat2)$ has been established. At the top part of Fig.6 (No Fuzzy Factor) it is possible to see the voltage at the DC bus at each ESS V_{Bat1} and V_{Bat2} when the fuzzy factor is not used. In the middle of Fig.6 it is possible to see the SoC with (continuous line) and without the fuzzy weight factor (dashed

line). Finally, at the bottom of Fig.6 (With Fuzzy Factor) it is possible to see the voltage at the DC bus at each ESS V_{Bat1} and V_{Bat2}, when the fuzzy factor is used.

The simulation time is split into 5 stages in order to indicate the changes at the operation mode of each RES and ESS. Table II summarizes the changes on the operation mode for each ESS and RES in accordance with times $T1$ to $T5$. It is possible to see from Fig.6 how the SoC of both ESS approaches asymptotically one to the other. Additionally, it is possible to see that the system with fuzzy weight factors reduce the depth of discharge of battery 1 and both batteries are charged faster taking into account that $T1 + T2 + T3$ is smaller when the fuzzy factor is used. Additionally, an undesirable situation is avoided when the fuzzy factor is used as can be seen at the beginning of $T5$. At this point, due to the difference at the instantaneous battery voltage, when the ESS start to provide power to the microgrid, a circulating current appears between the ESS. This fact may cause an excessive peak current for the battery array that may damage it.

Fig.7 shows the reactive and reactive power flow at each ESS and RES as well as the power in the load when the fuzzy factor is used. It is possible to see how the power flow regulation is exchanged between RES and ESS in accordance to the control operation mode summarized in Table II. At $T3$ battery 1 $(Bat1)$ become the only responsible of reactive
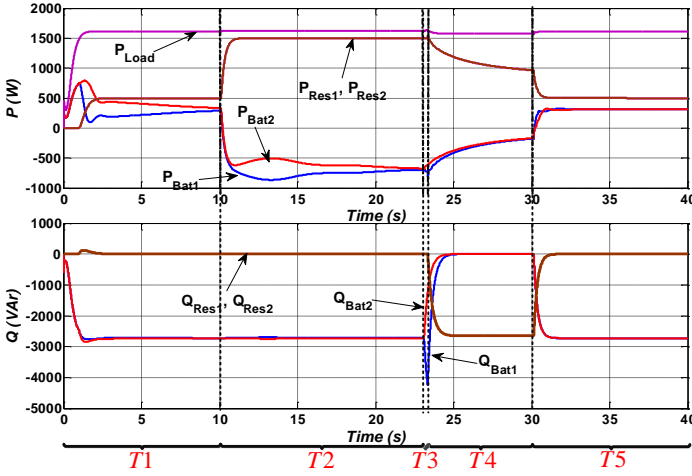
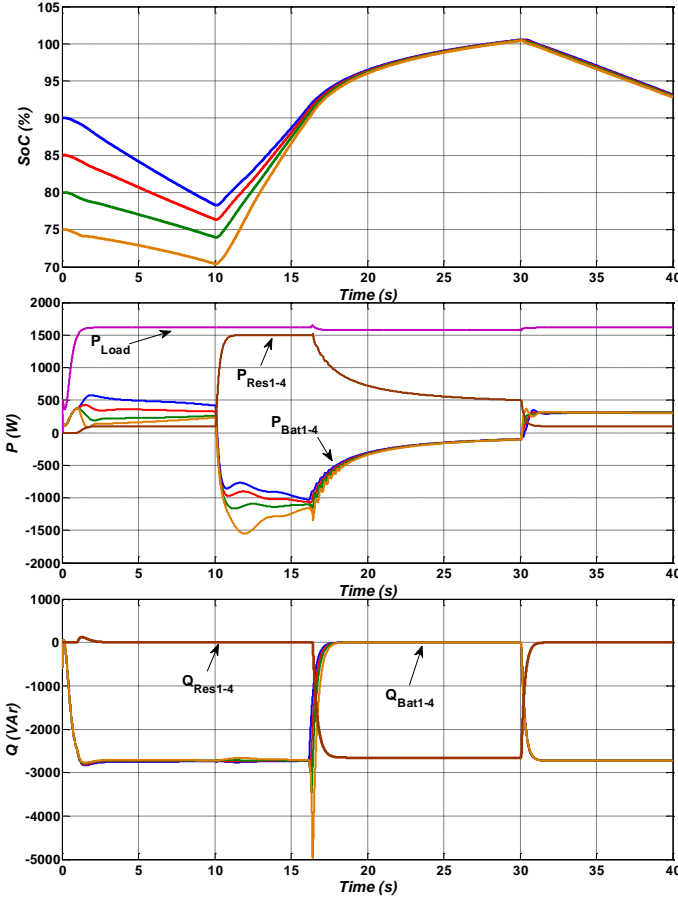Figure 7. Simulation results for P and Q power flow with fuzzy factor

Figure 8. Simulation results for 4 active generators in a AC microgrid

power flow, until it reach the regulation voltage. At this moment, all RES assume the reactive power flow regulation in a shared way. A power curtailment of the PV generation can be seen at $T4$, this curtailment is governed by the $(P-\omega)$ control loop in order to assure power sharing between RES.

Finally, Fig.8 shows the response of the microgrid (SoC, P and Q) when four active generators (PV+ESS) are used ($i = 4$). The results show that the proposed approach is completely expansible to several active power generators.

VI. CONCLUSION

The proposed adjustment of the droop coefficient by using a FIS, assures good storage energy balance for distributed ESS.

Additionally, this strategy is absolutely modular, expandable, and there is not required a centralized control. As a matter of fact, it can be used directly when a new active generator has to be added to the microgrid. Likewise, the proposed method shows additional advantages compared to traditional methods such as asymptotic approximation of the SoC for several ESS, faster charge in the total of distributed ESS and reduction of the deep of discharge for the ESS with the smallest SoC, among others. On top of that, the microgrid can operate in a stable and coordinated way under different scenarios without using communications.

REFERENCES

[1] D. Wu, F. Tang, T. Dragicevic, J. Vasquez, and J. Guerrero, "Autonomous active power control for islanded ac microgrids with photovoltaic generation and energy storage system," *Energy Conversion, IEEE Transactions on*, vol. PP, no. 99, 2014.

[2] H. Kanchev, D. Lu, F. Colas, V. Lazarov, and B. Francois, "Energy management and operational planning of a microgrid with a pv-based active generator for smart grid applications," *IEEE Transactions on Industrial Electronics*, vol. 58, pp. 4583–4592, Oct 2011.

[3] Y. Moumouni, Y. Baghzouz, and R. Boehm, "Power smoothing of a commercial-size photovoltaic system by an energy storage system," in *2014 IEEE 16th International Conference on Harmonics and Quality of Power (ICHQP)*, pp. 640–644, May 2014.

[4] J. de Matos, F. e Silva, and L. Ribeiro, "Power control in ac isolated microgrids with renewable energy sources and energy storage systems," *IEEE Transactions on Industrial Electronics,*, vol. PP, no. 99, pp. 1–1, 2014.

[5] C. Wang, M. Liu, and L. Guo, "Cooperative operation and optimal design for islanded microgrid," in *2012 IEEE PES Innovative Smart Grid Technologies (ISGT)*, pp. 1–8, Jan 2012.

[6] J. Cui, K. Li, Y. Sun, Z. Zou, and Y. Ma, "Distributed energy storage system in wind power generation," in *2011 4th International Conference on Electric Utility Deregulation and Restructuring and Power Technologies (DRPT)*, pp. 1535–1540, July 2011.

[7] F. Marra, G. Yang, C. Traeholt, J. Ostergaard, and E. Larsen, "A decentralized storage strategy for residential feeders with photovoltaics," *IEEE Transactions on Smart Grid*, vol. 5, pp. 974–981, March 2014.

[8] J. Guerrero, L. Garcia De Vicuna, J. Matas, M. Castilla, and J. Miret, "A wireless controller to enhance dynamic performance of parallel inverters in distributed generation systems," *IEEE Transactions on Power Electronics*, vol. 19, pp. 1205–1213, Sept 2004.

[9] J. Rocabert, A. Luna, F. Blaabjerg, and P. Rodríguez, "Control of power converters in ac microgrids," *IEEE Transactions on Power Electronics*, vol. 27, pp. 4734–4749, Nov 2012.

[10] N. Diaz, T. Dragicevic, J. Vasquez, and J. Guerrero, "Intelligent distributed generation and storage units for dc microgrids - a new concept on cooperative control without communications beyond droop control," *IEEE Transactions on Smart Grid*, vol. 5, pp. 2476–2485, Sept 2014.

[11] Y. Zhang, H. J. Jia, and L. Guo, "Energy management strategy of islanded microgrid based on power flow control," in *2012 IEEE PES Innovative Smart Grid Technologies (ISGT)*, pp. 1–8, Jan 2012.

[12] I. S. C. C. 21, "Ieee guide for optimizing the performance and life of lead-acid batteries in remote hybrid power systems," 2008.

[13] T. Dragicevic, J. Guerrero, J. Vasquez, and D. Skrlec, "Supervisory control of an adaptive-droop regulated dc microgrid with battery management capability," *IEEE Transactions on Power Electronics*, vol. 29, no. 2, pp. 695–706, 2014.

[14] X. Lu, K. Sun, J. Guerrero, J. Vasquez, L. Huang, and R. Teodorescu, "Soc-based droop method for distributed energy storage in dc microgrid applications," in *Industrial Electronics (ISIE), 2012 IEEE International Symposium on*, pp. 1640–1645, 2012.

[15] H. Kakigano, Y. Miura, and T. Ise, "Distribution voltage control for dc microgrids using fuzzy control and gain-scheduling technique," *Power Electronics, IEEE Transactions on*, vol. 28, no. 5, pp. 2246–2258, 2013.

[16] R. Babuska, *Fuzzy and Neuronal Control, Course Lecture Notes*. Delft University of Technology, 2009.

[17] E. Coelho, P. Cortizo, and P. Garcia, "Small-signal stability for parallel-connected inverters in stand-alone ac supply systems," *Industry Applications, IEEE Transactions on*, vol. 38, pp. 533–542, Mar 2002.